Original Article

MOLECULAR METABOLISM

TALK-1 reduces delta-cell endoplasmic reticulum and cytoplasmic calcium levels limiting somatostatin secretion

Nicholas C. Vierra, Matthew T. Dickerson, Kelli L. Jordan, Prasanna K. Dadi, Ketaki A. Kadare, Molly K. Altman, Sarah C. Milian, David A. Jacobson*

ABSTRACT

Objective: Single-cell RNA sequencing studies have revealed that the type-2 diabetes associated two-pore domain K^+ (K2P) channel TALK-1 is abundantly expressed in somatostatin-secreting δ-cells. However, a physiological role for TALK-1 in δ-cells remains unknown. We previously determined that in β-cells, K^+ flux through endoplasmic reticulum (ER)-localized TALK-1 channels enhances ER Ca^{2+} leak, modulating Ca^{2+} handling and insulin secretion. As glucose amplification of islet somatostatin release relies on Ca^{2+}-induced Ca^{2+} release (CICR) from the δ-cell ER, we investigated whether TALK-1 modulates δ-cell Ca^{2+} handling and somatostatin secretion.

Methods: To define the functions of islet δ-cell TALK-1 channels, we generated control and TALK-1 channel-deficient (TALK-1 KO) mice expressing fluorescent reporters specifically in δ- and α-cells to facilitate cell type identification. Using immunofluorescence, patch clamp electrophysiology, Ca^{2+} imaging, and hormone secretion assays, we assessed how TALK-1 channel activity impacts δ- and α-cell function.

Results: TALK-1 channels are expressed in both mouse and human δ-cells, where they modulate glucose-stimulated changes in cytosolic Ca^{2+} and somatostatin secretion. Measurement of cytosolic Ca^{2+} levels in response to membrane potential depolarization revealed enhanced CICR in TALK-1 KO δ-cells that could be abolished by depleting ER Ca^{2+} with sarco/endoplasmic reticulum Ca^{2+} ATPase (SERCA) inhibitors. Consistent with elevated somatostatin inhibitory tone, we observed significantly reduced glucagon secretion and α-cell Ca^{2+} oscillations in TALK-1 KO islets, and found that blockade of α-cell somatostatin signaling with a somatostatin receptor 2 (SSTR2) antagonist restored glucagon secretion in TALK-1 KO islets.

Conclusions: These data indicate that TALK-1 reduces δ-cell cytosolic Ca^{2+} elevations and somatostatin release by limiting δ-cell CICR, modulating the intraislet paracrine signaling mechanisms that control glucagon secretion.

Keywords Two-pore domain K^+ channel; *KCNK16*; Paracrine; Islet; Endoplasmic reticulum; Hormone secretion

1. INTRODUCTION

Somatostatin is a potent inhibitory peptide, which regulates many physiological processes, such as hormone secretion, neurotransmission, gastric function, and cell proliferation. Somatostatin signals through plasma membrane $G_{\alpha i}$-coupled receptors, suppressing cellular function through a number of mechanisms including inhibition of cAMP-dependent pathways and activation of inward-rectifier K^+ channels. In most cases, secreted somatostatin acts locally to regulate the activity of surrounding cells [1]. This is exemplified by intraislet somatostatin release, which inhibits glucagon and insulin secretion [2–4]. Islet somatostatin secretion is increased by elevated blood glucose levels [5], providing a paracrine feedback mechanism to curtail excessive insulin and glucagon secretion and minimize large fluctuations in glycemia. Although the necessity of proper islet somatostatin secretion for glucose homeostasis is increasingly appreciated, the molecular mechanisms underlying δ-cell function remain poorly understood. Emerging data suggest that dysregulated islet somatostatin secretion contributes to hyperglycemia in type 1 and type 2 diabetes mellitus (T2DM), highlighting the importance of determining the molecular physiology of δ-cells [2,6–9].

Somatostatin secretion requires extracellular Ca^{2+} influx through voltage-dependent Ca^{2+} channels (VDCCs) [10–12]. VDCC opening is determined by the plasma membrane potential (V_m), which is largely controlled by the activity of hyperpolarizing K^+ channels such as ATP-sensitive K^+ (K_{ATP}) channels. Pharmacological or metabolic inhibition of K_{ATP} channels stimulates Ca^{2+} entry and somatostatin secretion [3,9,13]. However, δ-cells lacking functional K_{ATP} channels still exhibit glucose-stimulated somatostatin secretion (GSSS), indicating that other mechanisms in addition to K_{ATP} channels contribute to GSSS [11]. Previous studies demonstrate that GSSS also relies upon paracrine stimulation by β-cells and Ca^{2+}-induced Ca^{2+} release (CICR) from the δ-cell ER [9,11]. CICR is sensitive to both cytoplasmic Ca^{2+} and total ER Ca^{2+} content [14–16]. Glucose metabolism accelerates

Department of Molecular Physiology and Biophysics, Vanderbilt University, Nashville, TN 37232, USA

*Corresponding author. Department of Molecular Physiology and Biophysics, Vanderbilt University, 7425B MRB IV, 2213 Garland Ave., Nashville, TN, 37232-0615, USA. E-mail: david.a.jacobson@vanderbilt.edu (D.A. Jacobson).

Received December 22, 2017 • Accepted January 19, 2018 • Available online 31 January 2018

https://doi.org/10.1016/j.molmet.2018.01.016

δ-cell sarco/endoplasmic reticulum Ca^{2+}-ATPase (SERCA) activity, resulting in elevated ER Ca^{2+} content, which enhances CICR [11]. Pharmacological inhibition of SERCA activity and subsequent depletion of ER Ca^{2+} significantly reduces somatostatin secretion, indicating that δ-cell ER Ca^{2+} stores serve a critical role in GSSS [11,17]. However, the mechanisms which govern δ-cell Ca^{2+} influx, ER Ca^{2+} stores, and CICR under different glucose conditions are largely unknown.

Recent studies demonstrate that the two-pore domain K^+ (K2P) channel TALK-1 (encoded by the *KCNK16* gene) is abundantly expressed in δ-cells of the islet and gastric epithelium [18–20]. Although the function of δ-cell TALK-1 channels remains unknown, β-cell TALK-1 channels control Ca^{2+} influx and insulin secretion by modulating electrical activity and ER Ca^{2+} homeostasis [21]. TALK-1 regulates β-cell ER Ca^{2+} handling by conducting K^+ countercurrents across the ER membrane which promote ER Ca^{2+} leak; inhibiting TALK-1 channel activity augments ER Ca^{2+} stores [22]. TALK-1 channels are also implicated in T2DM pathogenesis through a non-synonymous polymorphism (rs1535500, encoding TALK-1 A277E) which causes a gain-of-function in TALK-1 channel activity [21]. The rs1535500 polymorphism is associated with impaired insulin secretion in T2DM patients and increased T2DM susceptibility [23–27]. These data, along with the prominent expression of TALK-1 channels in the islet, suggest that defects in δ-cell function induced by TALK-1 A277E may contribute to islet dysfunction and exacerbate hyperglycemia in patients with T2DM. Given the role TALK-1 channels serve in regulating ER Ca^{2+} stores, prominent expression of TALK-1 mRNA in δ-cells, and sensitivity of CICR to ER Ca^{2+} levels, we investigated whether TALK-1 channels modulate δ-cell Ca^{2+} handling and somatostatin secretion. We found that TALK-1 forms functional channels in mouse and human δ-cells, where it limits CICR and somatostatin secretion. CICR and ER Ca^{2+} stores are enhanced in δ-cells lacking TALK-1 channels, leading to increased somatostatin secretion and reduced glucagon secretion. These findings highlight the physiological importance of TALK-1 channel modulation of δ-cell $Ca^{2+}{}_c$ homeostasis in regulating islet somatostatin signaling, and contribute to an improved understanding of the molecular mechanisms underlying GSSS.

2. MATERIALS AND METHODS

2.1. Chemicals

All chemicals were purchased from Sigma–Aldrich (St. Louis, MO) unless specified otherwise.

2.2. Biological materials and study approval

The mice used in this study were 10–15 week-old males on a C57Bl6/J background. Mice were housed in a 12-hour light/dark cycle with access to standard chow (Lab Diets, 5L0D) *ad libitum*. Wild-type (WT) and TALK-1 KO transgenic mice expressing tdRFP specifically in somatostatin-positive cells (RFP δ-cells) were generated by crossing mice expressing *Sst*-IRES-Cre [28] with mice expressing a tdRFP fluorescent reporter preceded by a loxP-flanked STOP cassette [29]. Transgenic mice expressing GCaMP6s specifically in somatostatin-positive cells were generated by crossing WT and TALK-1 KO mice expressing S*st*-IRES-Cre with those possessing the genetically encoded Ca^{2+} indicator GCaMP6s preceded by a loxP-flanked STOP cassette [36]. Mouse islets were isolated by digesting the pancreas with collagenase P (Roche) and performing density gradient centrifugation as previously described [30]. We obtained human islets from adult non-diabetic donors from multiple isolation centers organized by the Integrated Islet Distribution Program (human islet donor characteristics are provided in Table S1). Mouse and human islets were cultured in RPMI 1640 (Gibco) containing 15% fetal bovine serum (FBS), 100 IU·ml^{-1} penicillin, and 100 mg ml^{-1} streptomycin, in an incubator maintained at 37 °C, 5% CO_2. Although the concentration of glucose in RPMI 1640 (11 mM) is higher than typical resting glucose in humans (5.6 mM), human cells are more amenable to patch clamp recording when cultured under these conditions. Moreover, we do not observe significant differences in δ-cell electrical excitability when cultured with high (11 mM) and low (1 mM) glucose. Islets and cells were seeded to poly-D-lysine-coated 35 mm glass-bottom dishes (CellVis). In experiments using single islet cells, islets were triturated in 0.0075% trypsin-EDTA prior to plating. Dispersed cells were cultured for approximately 6 h in 100 μL of medium prior to being refed with 2 mL of fresh medium. In human δ-cell experiments, cells were transfected with TALK-1 DN- or mCherry-expressing plasmids and identified by post-staining for somatostatin as previously described [21]. Briefly, cells were transfected for 18 h using 1 μL Lipofectamine 3000 and 1 μL P3000 (Thermo Fisher) with 400 ng DNA in a total volume of 100 μL of the transfection mixture. After 18 h the cells were re-fed with fresh media. For Ca^{2+} imaging experiments using primary human δ-cells, cells were infected 48 prior to imaging with Psst-mCherry adenovirus to facilitate identification of δ-cells [31]. All mouse procedures performed in this study were done in compliance with protocols reviewed and approved by the Vanderbilt University Institutional Animal Care and Use Committee, according to guidelines set forth by the National Institutes of Health.

2.3. Immunofluorescence

Paraffin-embedded mouse and human pancreas sections were processed and stained as previously described (human donor information is provided in Table S2) [21]. Sections were stained using primary antibodies against somatostatin (Santa Cruz Biotechnology sc-7819: 1:250), TALK-1 (Novus Biologicals #NBP1-83071; 1:175) or TALK-1a (Antibody Verify AAS72353C; 1:250), glucagon (Proteintech #15954-I-AP: 1:500), and the endoplasmic reticulum marker GRP94 (Novus Biologicals #NB300-619; 1:100); secondary antibodies used were Alexa Fluor 488-conjugated donkey anti-rabbit (Jackson Immunoresearch #711-546-152; 1:300), DyLight 650-conjugated donkey anti-goat (Thermo Fisher #SA5-10089; 1:250), and Cy3-conjugated donkey anti-mouse (Jackson Immunoresearch #715-166-150; 1:500).

2.4. Calcium imaging

Ca^{2+} imaging was performed as previously described using epifluorescent or confocal miscroscopy with Ca^{2+} dyes (Fura-2 AM, Cal520-AM, or Cal590-AM) or genetic indicators (GCaMP3 or GCaMP6s) [22]. Further details on the protocols used to measure $Ca^{2+}{}_c$ can be found in the supplemental data.

2.5. Cross-correlation analysis

The glucose-mediated synchronization of islet β- and δ-cell Ca^{2+} oscillations was calculated using the cross-correlation function of Clampfit 10. Changes in the GCaMP6s signal of individual δ-cells within an islet were correlated to Cal590-AM signal in the same islet at 1 mM glucose, 11 mM glucose, and 11 mM glucose with 50 μM CPA. As Cal590-AM was utilized as an indicator of β-cell $Ca^{2+}{}_c$, areas displaying GCaMP6s fluorescence were excluded from analysis. Correlation coefficients for β-cell/δ-cell synchronization were determined as a function of lag time between Cal590-AM and δ-cell GCaMP6s signals [32].

2.6. Patch clamp electrophysiology

An Axopatch 200B amplifier (Molecular Devices) was used to measure whole-cell K^+ channel currents in the voltage-clamp mode; currents

were digitized using a Digidata 1440, lowpass filtered at 1 kHz and sampled at 10 kHz. During recording, samples were perfused with KRB without $CaCl_2$ and supplemented with (in mM): 0.2 tolbutamide (MP Biomedicals), 10 tetraethylammonium chloride hydrate (TEA, Thermo Fisher Scientific), 1 EGTA, pH 7.35 with NaOH, and 11 mM glucose. Patch electrodes were pulled to a resistance of 3–4 MΩ and filled with an intracellular solution containing (in mM): 140 KCl, 1 $MgCl_2$, 10 EGTA, 10 HEPES, and 3 Mg-ATP, pH 7.22 with KOH. For V_m recordings, pipettes were filled with an intracellular solution containing (in mM) 28.4 K_2SO_4, 63.7 KCl, 11.8 NaCl, 1 $MgCl_2$, 20.8 HEPES, 0.5 EGTA (pH 7.22 with KOH) and ~0.05 mg ml^{-1} amphotericin B. δ-cells were continuously perfused with KRB solutions at 35–36 °C. VDCC currents were recorded from dispersed mouse δ-cells as previously described [33]. Patch electrodes were pulled to a resistance of 3–4 MΩ when filled with an intracellular solution containing (in mM): 120 CsCl, 10 TEA, 1 $MgCl_2$, 3 EGTA, 10 HEPES, 3 MgATP, pH 7.22 with CsOH. Cells were patched in KRB solution supplemented with 11 mM glucose; upon obtaining the whole-cell configuration with a seal resistance >1 GΩ, the bath solution was exchanged for a buffer containing (in mM): 82 N-methyl-D-glucamine, 20 TEA, 30 $CaCl_2$, 1 $MgCl_2$, 5 CsCl, 10 HEPES, 11 glucose, 0.2 tolbutamide, pH 7.35 with HCl, osmolarity adjusted with sucrose. δ-cells were perfused for 3 min with this solution prior to initiating the VDCC recording protocol. Voltage steps of 10 mV were applied from a holding potential of −80 mV; linear leak currents were subtracted online using a *P*/4 protocol. Data were analyzed using Clampfit 10 and Microsoft Excel.

2.7. Hormone secretion

For all experiments, islets were allowed to recover for 24 h following isolation in RPMI 1640 supplemented with 15% FBS and 11 mM glucose. Glucagon secretion was then determined by radioimmunoassay from perifused islets stimulated with 1 and 11 mM glucose (Vanderbilt Islet Procurement & Analysis Core; supported by the Vanderbilt Diabetes Research and Training Center; P60 DK020593) [21]. Glucagon and somatostatin secretion measurements from static incubations were performed as previously described [34]. Somatostatin was measured using a fluorescent EIA kit according to the manufacturer's instructions (Phoenix Pharmaceuticals #FEK-060-03).

2.8. Statistical analysis

The data are shown as recordings that are averaged or representative of results obtained from at least three independent cultures. The values presented are the mean ± SE. Statistical differences between means were assessed using two-tailed unpaired Student's *t*-test unless stated otherwise. A $P < 0.05$ was considered as significant.

3. RESULTS

3.1. TALK-1 channels are expressed in δ-cells

We first sought to determine whether functional TALK-1 channels are expressed in the ER of δ-cells. Somatostatin-positive cells from mouse and human pancreas sections displayed strong intracellular localization of TALK-1, which resembled the staining pattern for an ER marker (GRP94). This suggests that, as with β-cells, TALK-1 may serve a role in the ER of islet δ-cells (Figure 1A–D) [22]. As TALK-1 expression has also been reported in gastric δ-cells [19], we stained paraffin embedded sections of human duodenum and stomach for TALK-1 and somatostatin. In agreement with transcriptome analyses, TALK-1 was detectable in gastric somatostatin-positive cells (Figs. S1A,B). We next went on to test whether TALK-1 forms functional K^+ channels in mouse islet δ-cells using TALK-1 deficient mice (TALK-1 KO) [21]. We dispersed these islet cell preparations and recorded whole-cell K2P currents from single RFP δ-cells, which were significantly reduced in δ-cells from TALK-1 KO mice when compared to WT (Figure 1E). To assess whether TALK-1 also forms a functional channel in human δ-cells, we expressed a TALK-1 dominant-negative (DN) mutant to inhibit endogenous TALK-1 channel activity [21]. The TALK-1 DN relies on a mutation (G110E) in the K^+ selectivity filter that abolishes K^+ conductance upon interaction with wild-type TALK-1; the TALK-1 DN construct also possesses an mCherry fluorescent reporter separated from TALK-1 DN by a P2A sequence, facilitating identification of transfected cells [21]. Expression of the TALK-1 DN in single human δ-cells (confirmed by post-staining for somatostatin) resulted in inhibition of whole-cell K2P currents (Figure 1F). These observations indicate that TALK-1 forms K^+ channels in δ-cells.

Physiological δ-cell function depends upon the islet microenvironment which enables paracrine feedback mechanisms between β-, α-, and δ-cells [9,35,36]. Therefore, we also examined how TALK-1 channel activity impacts δ-cell cytosolic Ca^{2+} (Ca^{2+}_c) homeostasis in intact islets. This was accomplished by crossing our TALK-1 KO/*Sst*-IRES-Cre mice with those possessing the genetically encoded Ca^{2+} indicator GCaMP6s preceded by a loxP-flanked STOP cassette [37], generating islets with GCaMP6s expressed specifically in δ-cells. As δ-cell Ca^{2+}_c has been reported to oscillate in synchrony with β-cells [31], we loaded GCaMP6s-expressing islets with the red synthetic Ca^{2+} indicator Cal590-AM to examine the relationship between β- and δ-cell Ca^{2+}_c in whole islets. As approximately 85% of islet cells are β-cells, total islet Cal590-AM signal excluding GCaMP6s positive δ-cells was monitored as an indicator of β-cell Ca^{2+}_cresponse [38]. In low (1 mM) glucose there was no coordination between β- and δ-cell Ca^{2+}_coscillations as 66.4 ± 3.9% WT and 70.0 ± 6.4% TALK-1 KO δ-cells exhibited Ca^{2+}_c oscillations (Figure 2A–C,F, and K), whereas β-cells remained quiescent. Under high (11 mM) glucose, nearly all δ-cells responded with increased Ca^{2+}_cthat correlated with β-cell Ca^{2+}_coscillations (Figure 2D,G). In TALK-1 KO islets, islet Ca^{2+}_coscillation frequency is significantly accelerated [21], and this phenotype was also observed in TALK-1 KO δ-cells in intact islets (Figure 2I). We also found that intact islet TALK-1 KO δ-cells produced larger amplitude Ca^{2+}_c oscillations compared to WT δ-cells under both low and high glucose conditions (Figure 2J). In WT and TALK-1 KO δ-cells, glucose increased the amplitude of Ca^{2+}_c oscillations, consistent with observations that glucose metabolism enhances δ-cell CICR [11]. The height of the Ca^{2+}_c oscillations in elevated glucose was reduced to the amplitude observed in low glucose by depleting ER Ca^{2+} with the SERCA inhibitor CPA (Figure 2J) [22,39,40]. Interestingly, following the addition of CPA Ca^{2+}_c oscillations ceased in β-cells but continued in a sub-population of δ-cells indicating a decrease in glucose-induced coupling between β- and δ-cells (Figure 2E,H). This suggests that ER Ca^{2+} handling may be involved in this relationship.

We next investigated whether the absence of TALK-1 channels altered Ca^{2+}_c handling in single δ-cells. Using dispersed islet-cells, we monitored single δ-cell Ca^{2+}_c under stimulatory (11 mM) glucose conditions in WT and TALK-1 KO δ-cells (Figure 3A,B). Under these conditions, both WT and TALK-1 KO δ-cells exhibited oscillations in Ca^{2+}_c. Area under the Ca^{2+} curve (AUC) analysis between 0 and 800 s revealed that under these conditions the change in Ca^{2+}_c was significantly greater in TALK-1 KO δ-cells as compared to WT δ-cells (Figure 3C); a difference which was abolished by removal of extracellular Ca^{2+} (AUC was analyzed between 1300 and 1500 s). The amplitude of δ-cell Ca^{2+} transients was also significantly greater in TALK-1 KO islets (Figure 2J) and in single TALK-1 KO δ-cells (Figure 3D) than in corresponding WT islets and WT δ-cells. As an

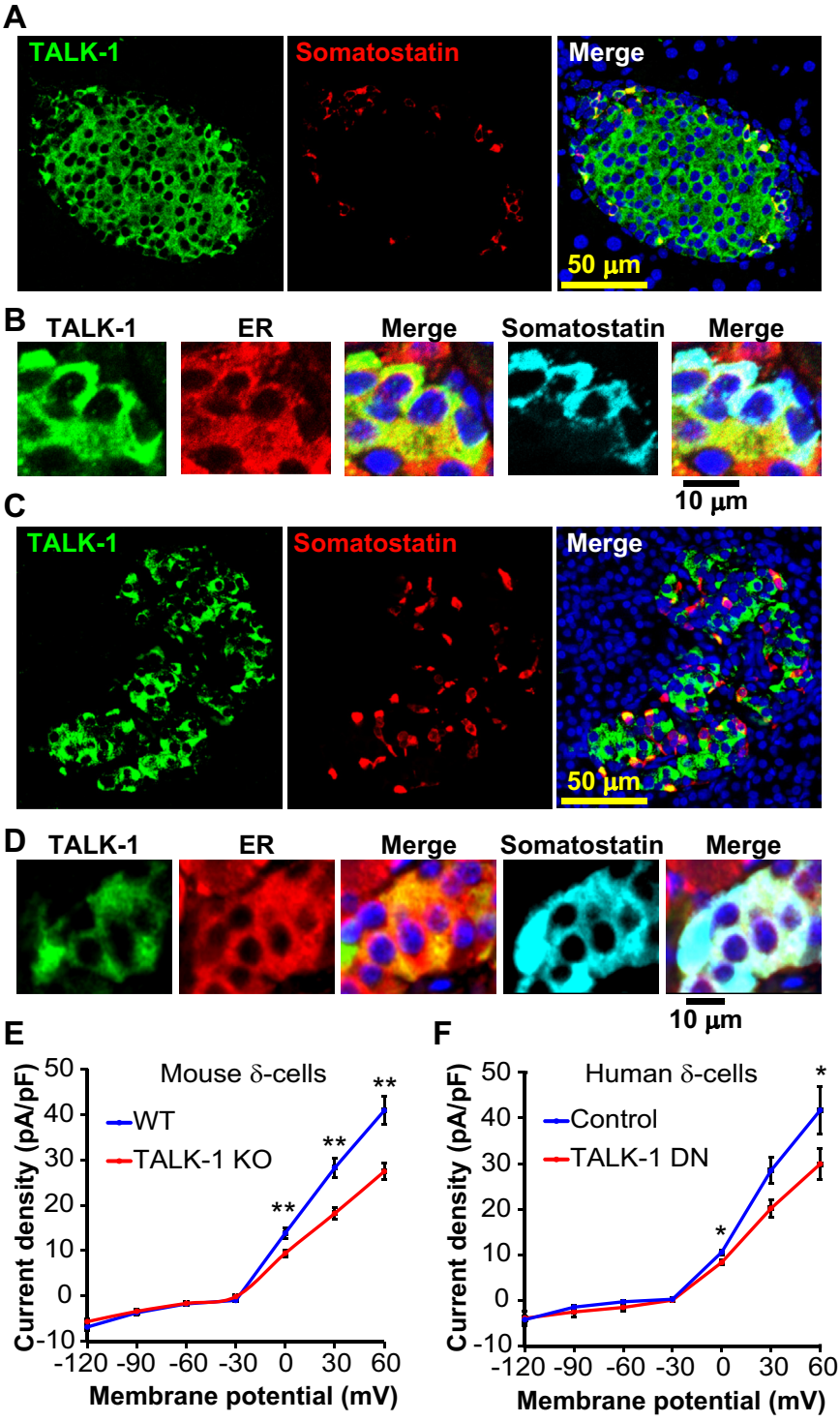

Figure 1: TALK-1 channels are expressed in mouse and human δ-cells. (A) Mouse pancreas section stained for TALK-1 (green) and somatostatin (red) (representative of $N = 3$ mice). (B) Mouse pancreas section stained for TALK-1 (green), ER (GRP94, red), and SST (cyan). (C) Human pancreas section stained for TALK-1 (green) and somatostatin (red) (representative of $N = 3$ pancreata). (D) Human pancreas section stained for TALK-1 (green), ER (GRP94, red), and somatostatin (E) K2P currents recorded from WT and TALK-1 KO δ-cells ($N = 3$ mice per genotype). (F) K2P currents recorded from human δ-cells expressing TALK-1 DN or control mCherry. ($N = 3$ islet preparations); $^{*}P < 0.05$, $^{**}P < 0.005$.

elevation $Ca^{2+}{}_c$ is critical for somatostatin secretion, we went on to measure somatostatin release from WT and TALK-1 KO islets. Compared to WT islets, somatostatin secretion was increased by approximately 20% under basal (1 mM glucose) conditions and enhanced by over 60% under stimulatory (11 mM glucose) conditions from islets lacking TALK-1 (Figure 3E).

GSSS relies on glucose metabolism, and inhibition of glucose metabolism significantly reduces depolarization-induced somatostatin

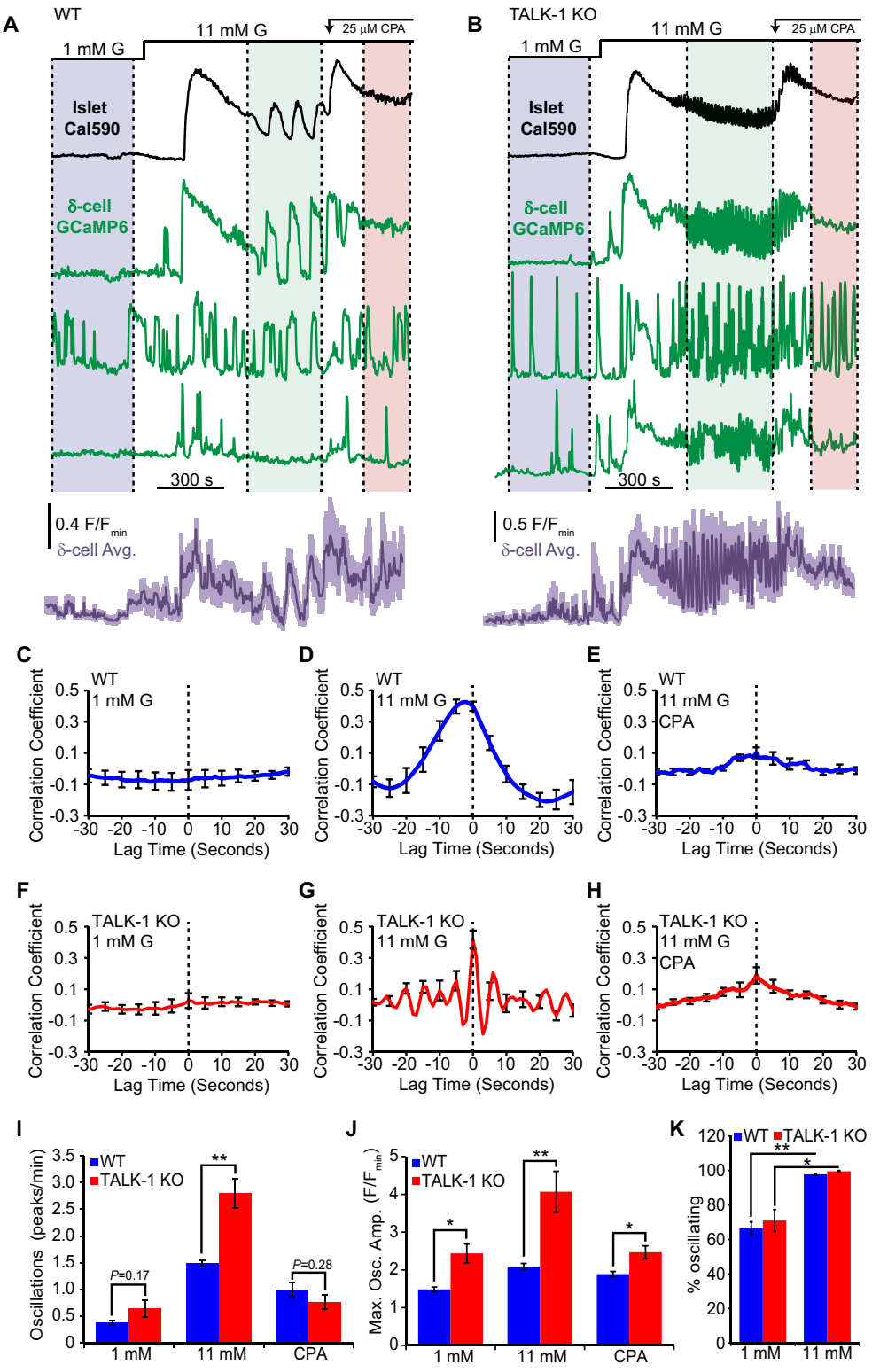

Figure 2: Glucose synchronizes WT and TALK-1 KO δ-cell $Ca^{2+}{}_c$ with β-cells. (A) Recording of $Ca^{2+}{}_c$ from a WT islet expressing GCaMP6s in δ-cells and loaded with the red Ca^{2+} dye Cal590-AM (black: representative WT islet Cal590-AM signal excluding GCaMP6s-positive δ-cells, green: representative WT δ-cell GCaMP6s signals, purple: average WT δ-cell GCaMP6s signal; lines above indicate glucose concentrations; colored regions delineate periods used for cross-correlation analysis). (B) Recording of $Ca^{2+}{}_c$ from a TALK-1 KO islet expressing GCaMP6s in δ-cells and loaded with the red Ca^{2+} dye Cal590-AM (black: representative TALK-1 KO islet Cal590-AM signal excluding GCaMP6s-positive δ-cells, green: representative TALK-1 KO δ-cell GCaMP6s signals, and purple: average TALK-1 KO δ-cell GCaMP6s signal). (C) Average correlation between WT β- and δ-cells at 1 mM glucose ($N = 13$ islets). (D) Average correlation between WT β- and δ-cells at 11 mM glucose ($N = 13$ islets). (E) Average correlation between WT β- and δ-cells at 11 mM glucose + 50 μM CPA ($N = 13$ islets). (F) Average correlation between TALK-1 KO β- and δ-cells at 1 mM glucose ($N = 12$ islets). (G) Average correlation between TALK-1 KO β- and δ-cells at 11 mM glucose ($N = 12$ islets). (H) Average correlation between TALK-1 KO β- and δ-cells at 11 mM glucose + 50 μM CPA ($N = 12$ islets). (I). Average δ-cell Ca^{2+} oscillation frequency in WT and TALK-1 KO δ-cells measured under the indicated conditions ($N = 3$ mice per genotype). (J) Average maximum GCaMP6s fluorescence amplitude in WT and TALK-1 KO δ-cells measured under the indicated conditions ($N = 3$ mice per genotype). (K) Comparison of percent of δ-cells exhibiting Ca^{2+} oscillations under indicated glucose conditions ($N = 3$ mice per genotype); $^*P < 0.05$; $^{**}P < 0.005$.

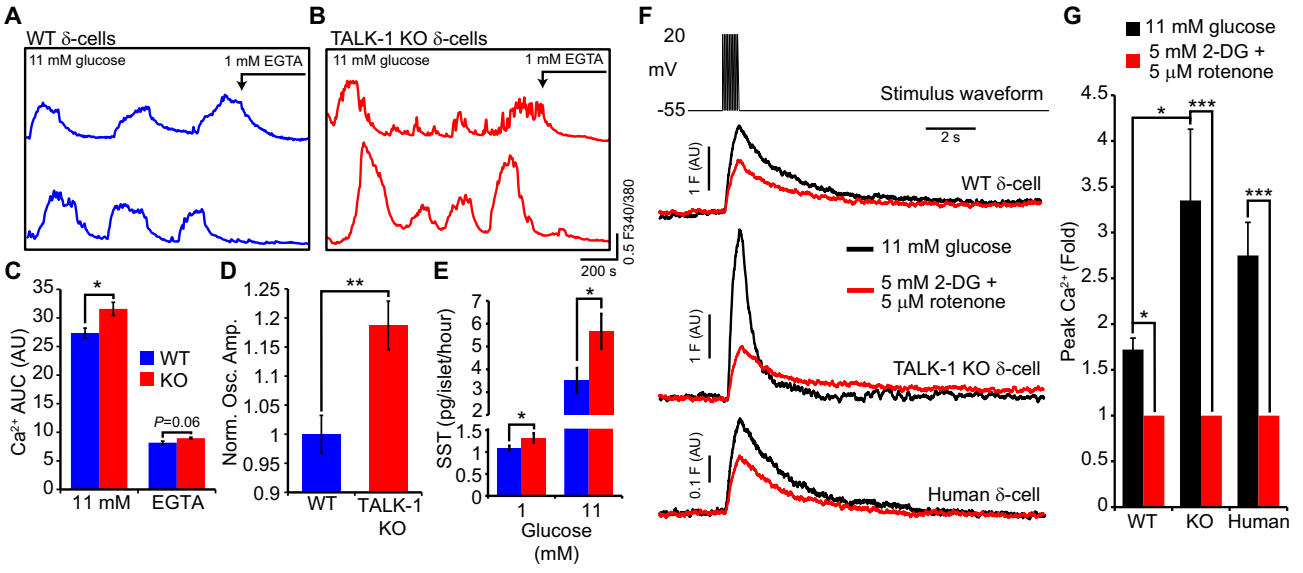

Figure 3: TALK-1 limits changes in δ-cell Ca^{2+}_c and somatostatin secretion. (A) Ca^{2+}_c recorded in single Fura-2-loaded WT δ-cells perfused with the indicated treatments (representative of $N = 3$ mice per genotype). (B) Ca^{2+}_c recorded in single Fura-2-loaded TALK-1 KO δ-cells perfused with the indicated treatments (representative of $N = 3$ mice per genotype). (C) Increase in Ca^{2+}_c (area under the curve, AUC) in WT and TALK-1 KO δ-cells (AUC with 11 mM glucose was quantified between 0 and 800 s and AUC with EGTA and no extracellular Ca^{2+} was quantified between 1300 and 1500 s; $N = 3$ mice per genotype). (D) Maximum Ca^{2+}_c oscillation amplitude (F/F_{min}) measured in WT and TALK-1 KO δ-cells ($N = 6$ mice per genotype). (E) Somatostatin secretion from WT and TALK-1 KO islets at 1 and 11 mM glucose ($N = 4$–7 islet preparations per genotype). (F) Representative Ca^{2+}_c transients in WT, TALK-1 KO, and human δ-cells subjected to depolarizing pulses in the presence of 11 mM glucose or 5 mM 2-deoxyglucose and 5 μM rotenone. The fold increase in δ-cell Ca^{2+} in response to increasingly is quantified in (G) ($N = 12$ cells (WT); 12 cells (TALK-1 KO); 7 cells (human)). $^*P < 0.05$, $^{**}P < 0.005$, $^{***}P < 0.0005$; ANOVA followed by Tukey's multiple comparison test.

secretion [11]. To assess how glucose metabolism contributes to the amplification of δ-cell Ca^{2+}_c transients, we measured depolarization-induced Ca^{2+}_c changes in patch-clamped single δ-cells. Application of 2-deoxyglucose, which inhibits glycolysis, and rotenone, which limits mitochondrial ATP synthesis, reduced the increase in Ca^{2+}_c following depolarization in control, TALK-1 KO, and human δ-cells (Figure 3F,G). Additionally, the reduction in Ca^{2+}_c transient amplitude caused by inhibition of glucose metabolism was significantly greater in TALK-1 KO δ-cells when compared to controls, suggesting that TALK-1 channels limit elevations in δ-cell Ca^{2+}_c. Interestingly, δ-cell Ca^{2+}_c returned to baseline more rapidly following depolarization in TALK-1 KO compared to WT δ-cells. This may be due to enhanced CICR in TALK-1 KO δ-cells, which would be expected to lead to a greater drop in ER Ca^{2+} in TALK-1 KO compared to WT δ-cells. As SERCAs are activated by depletion of ER Ca^{2+} [41,42], SERCA activity would presumably be higher in TALK-1 KO δ-cells resulting in faster removal of Ca^{2+} from the cytoplasm. Taken together, these observations indicate that δ-cell TALK-1 channels regulate δ-cell Ca^{2+}_c, demonstrate that there is significant crosstalk between β-cells and δ-cells under glucose conditions which stimulate β-cell Ca^{2+} influx, and confirm that glucose metabolism exerts an amplifying effect on δ-cell Ca^{2+}_c.

3.2. TALK-1 KO δ-cells are modestly depolarized

As TALK-1 produces detectable K^+ currents at the plasma membrane in δ-cells, we next investigated electrical activity in TALK-1 KO δ-cells. Islets were dispersed into clusters of cells to ensure accurate positioning of the recording pipette on RFP δ-cells. In both WT and TALK-1 KO δ-cells, we found that the V_m was largely insensitive to changes in extracellular glucose (Figure 4A–E), with action potential firing in low (1 mM) glucose. Similarly, we found no significant difference in the plateau fraction (the ratio of time spent in electrically excitable periods divided by the total time examined) comparing either the effects of glucose or genotype (Figure 4C). TALK-1 KO δ-cells were slightly depolarized in high glucose during electrically silent periods (Figure 4D), but we detected no difference in the plateau V_m from which action potentials fire (Figure 4E). There were also no appreciable differences in the pattern or frequency of action potentials in TALK-1 KO δ-cells when compared to WT δ-cells; however, action potential upstroke and afterhyperpolarization (AHP) had larger amplitudes in KO δ-cells (Table 1). We also measured VDCC currents to assess whether changes in Ca^{2+} channel function could account for the greater change in Ca^{2+}_c in TALK-1 KO δ-cells. However, we found no difference in VDCC currents (Figure 4F,G), indicating that alterations in VDCCs per se are unlikely a major source of increased Ca^{2+}_c in TALK-1 KO δ-cells. Thus, we went on to assess whether the increased Ca^{2+}_c observed in TALK-1 KO δ-cells was due to altered intracellular Ca^{2+} handling.

3.3. CICR is enhanced in TALK-1 KO δ-cells

One of the mechanisms proposed to underlie the glucose-induced increase in somatostatin secretion is enhanced CICR [11]. As TALK-1 channels modulate ER Ca^{2+} content, we examined whether elevated Ca^{2+}_c in TALK-1 KO δ-cells was a consequence of increased CICR. First, we determined whether ER Ca^{2+} stores were increased in δ-cells lacking TALK-1 channels by measuring CPA-induced ER Ca^{2+} release. Based on δ-cell current clamp V_m recordings, the impact of TALK-1 at the plasma membrane on ER Ca^{2+} levels was predicted to be minimal; however, to eliminate this possibility Ca^{2+} influx was clamped with high K^+ and diazoxide prior to removal of Ca^{2+} from the recording solution. Similar to our observations in TALK-1 KO β-cells [22], ER Ca^{2+} stores were higher in TALK-1 KO δ-cells (WT: 22.9 ± 4.5 AUC and TALK-1 KO: 35.7 ± 4.4 AUC, $P < 0.005$, Figs. S2A,B). The CPA-induced rate of ER Ca^{2+} release was also accelerated in TALK-1 KO compared to WT δ-cells (Fig. S2C). To

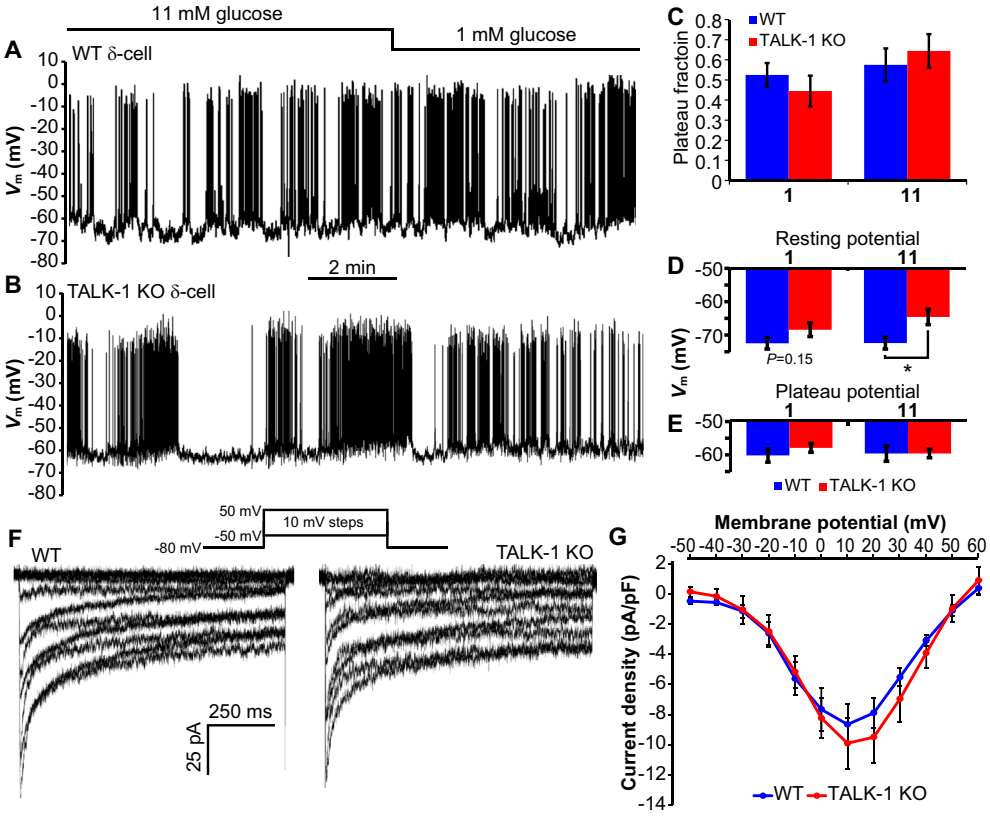

Figure 4: Electrical activity and VDCC currents in WT and TALK-1 KO δ-cells. (A) V_m recording from a WT δ-cell treated with indicated glucose concentrations (representative of recordings obtained from $N = 12$ cells/4 mice per genotype). (B) V_m recording from a TALK-1 KO δ-cell treated with indicated glucose concentrations (representative of recordings obtained from $N = 12$ cells/4 mice per genotype). (C) Quantification of plateau fraction in WT and TALK-1 KO δ-cells ($N = 12$ cells/4 mice per genotype). (D and E) Average V_m in WT and TALK-1 δ-cells at 1 and 11 mM glucose. ($N = 12$ cells/4 mice per genotype). (F) VDCC currents recorded from WT (representative of $N = 9$ cells/3 mice per genotype) and TALK-1 KO (representative of $N = 8$ cells/3 mice per genotype) δ-cells. VDCC current densities are quantified in (G); $^*P < 0.05$.

further examine δ-cell Ca^{2+} handling independent of glucose-induced changes in the V_m, we treated single WT and TALK-1 KO δ-cells with a solution containing 11 mM glucose to energize SERCAs and the K_{ATP} channel activator diazoxide to suppress electrical excitability. Under these conditions $Ca^{2+}{}_c$ oscillations were mostly abolished, but a 40-second depolarization with high (45 mM) K^+ elicited a rapid increase in $Ca^{2+}{}_c$ that slowly returned to basal levels upon removal of the depolarizing K^+ stimulus (Figure 5A,B). To investigate the contribution of the ER to changes in $Ca^{2+}{}_c$ under these conditions, we repeated this experiment in δ-cells pre-treated with the SERCA inhibitor thapsigargin (Figure 5A,B). Subtraction of the $Ca^{2+}{}_c$ signal obtained from thapsigargin-treated cells from the $Ca^{2+}{}_c$ signal of vehicle-treated cells revealed that depolarization induces a transient uptake of $Ca^{2+}{}_c$ by the ER followed by ER Ca^{2+} release (Figure 5C), similar to observations in β-cells [43]. In δ-cells, ER Ca^{2+} release preceded the end of the high K^+ pulse and was substantially greater in TALK-1 KO compared to WT δ-cells (Figure 5C). Similarly, we observed a larger rise in $Ca^{2+}{}_c$ in TALK-1 KO δ-cells compared to WT δ-cells when K_{ATP} was activated with diazoxide and Ca^{2+} was clamped with high K^+ for several minutes (WT:422.8 ± 62.6 AUC and TALK-1 KO: 953.3 ± 78.9 AUC, $P < 0.01$, Figure 5D). This is consistent with past reports that documented sustained CICR over a period of several minutes in the presence of a stimulus [44,45]. To determine whether increased ER Ca^{2+} release in TALK-1 KO δ-cells is a consequence of enhanced CICR, we next used fast imaging to measure $Ca^{2+}{}_c$ changes in patch-clamped δ-cells. 25–250 ms step depolarizations (−80 mV–0 mV) induced prompt increases in $Ca^{2+}{}_c$ which decayed to basal levels upon stepping back to the pre-pulse potential (Figure 5E). The depolarization-induced increases in $Ca^{2+}{}_c$ were significantly greater in TALK-1 KO δ-cells, a difference which could be eliminated by depleting ER Ca^{2+} with CPA to indirectly preclude CICR (Figure 5F). As these data suggested that enhanced CICR contributes to elevated $Ca^{2+}{}_c$ in TALK-1 KO δ-cells, we assessed whether depleting ER Ca^{2+} with CPA would return glucose-stimulated $Ca^{2+}{}_c$ in KO δ-cells to a level comparable to WT δ-cells (Figure 5G). Indeed, whereas $Ca^{2+}{}_c$ levels were significantly higher in TALK-1 KO δ-cells in 11 mM glucose (Figure 5G [see also Figures 2J, 3C, and 3D]), CPA treatment resulted in comparable $Ca^{2+}{}_c$ levels in WT and TALK-1 KO δ-cells. Interestingly, although ER Ca^{2+} depletion with a SERCA inhibitor suppressed glucose-stimulated somatostatin release [11,17] and $Ca^{2+}{}_c$ oscillation amplitude (Figure 2F), CPA treatment paradoxically

Table 1: – Action potential characteristics in WT and TALK-1 KO δ-cells. Action potential parameters were determined over a period of 60 s in the second oscillation of electrical activity in δ-cells treated with 11 mM glucose and are reported relative to the plateau V_m ($N = 12$ cells/3 mice per genotype).

Parameter	WT	TALK-1 KO	*P* value
Peak amplitude (mV)	40.8 ± 1.3	51.0 ± 2.7	0.002
AHP amplitude (mV)	−5.3 ± 0.7	−6.9 ± 0.4	0.05
Event frequency (Hz)	1.5 ± 0.2	1.7 ± 0.2	0.36

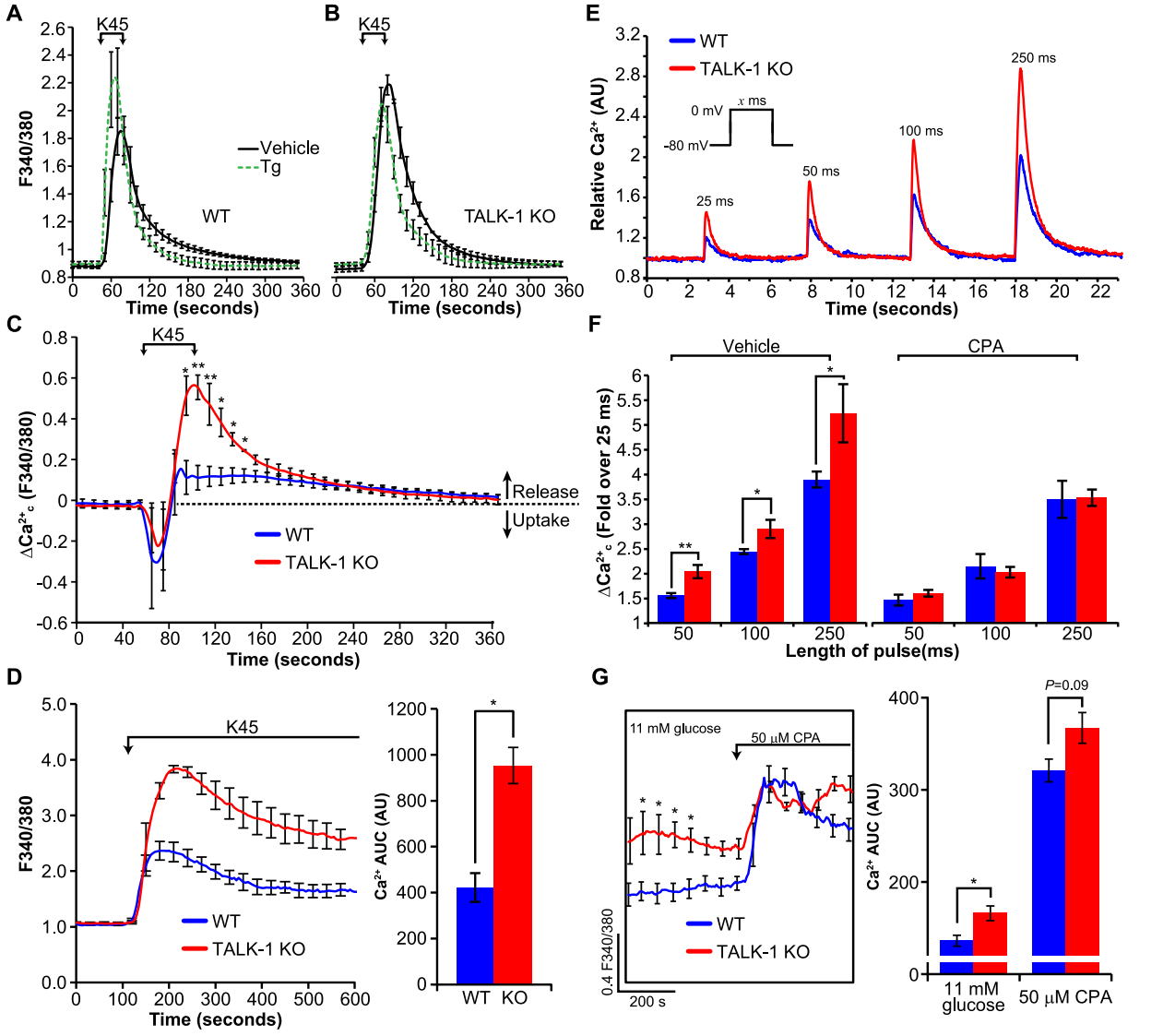

Figure 5: CICR is increased in TALK-1 KO δ-cells. (A, B) Average increase in Ca^{2+}_c following high K^+ (45 mM)-induced depolarization in WT and TALK-1 KO δ-cells, treated with vehicle or with 5 μM thapsigargin (Tg). SERCAs were energized with 11 mM glucose and K_{ATP} was activated with 125 μM diazoxide. Subtraction of the signal obtained from Tg treated cells from vehicle treated cells reveals the contribution of the ER to the Ca^{2+}_c signal (C) ($N = 3$ mice per genotype). (D) Average change in Ca^{2+}_c in response to treatment with diazoxide (125 μM) and depolarization with 45 mM K^+ in WT and TALK-1 KO δ-cells ($N = 3$ mice per genotype); $^*P < 0.05$. (E) Representative Ca^{2+}_c transients in WT and TALK-1 KO δ-cells subjected to short depolarizing pulses. The fold increase in δ-cell Ca^{2+} in response to increasingly long depolarizations in the presence or absence of CPA (25 μM) is quantified in (F) ($N = 9$ cells (WT); 7 cells (TALK-1 KO); 3 mice per genotype). (G) Ca^{2+}_c in WT and TALK-1 KO δ-cells was assessed before and after treatment with CPA. ($N = 3$ mice per genotype); $^*P < 0.05$, $^{**}P < 0.005$.

elevated bulk δ-cell Ca^{2+}_c levels (Figure 5G). The CPA-induced elevation in average δ-cell Ca^{2+}_c may be due to V_m depolarization caused by activation of store-operated currents (SOCs). Indeed, in the presence of V_m-hyperpolarizing diazoxide, basal Ca^{2+}_c in thapsigargin-treated δ-cells was not elevated (Figure 5A,B). These observations suggest that SOCs regulate δ-cell Ca^{2+}_c by modulating the V_m and VDCCs, and highlight that somatostatin secretion is very sensitive to ER Ca^{2+} release.

3.4. Glucagon secretion is reduced from TALK-1 KO islets

The acute sensitivity of α-cells to somatostatin under low glucose conditions is highlighted by the several-fold increase in glucagon secretion when somatostatin signaling is blocked [3,46,47]. Thus, somatostatin exerts an inhibitory tone on α-cells in low glucose, and increased basal somatostatin secretion leads to reduced glucagon secretion [3]. In TALK-1 KO islets, we found that glucagon release is significantly impaired under low glucose conditions (Figure 6A–C). While RNA sequencing of sorted α-cells has revealed high levels of *KCNK16* mRNA (gene encoding TALK-1), TALK-1 protein is not detected in mouse or human α-cells [8,21,48,49]. It is not clear why *KCNK16* mRNA is present in α-cells but not TALK-1 protein; however, Blodgett and colleagues also observed high levels of insulin mRNA but not protein in α-cells [48]. These observations underscore the importance of functional experimentation in support of transcriptome analysis and that the molecular mechanisms regulating islet-cell hormone mRNA expression are still incompletely understood. To further verify the absence of TALK-1 channels in α-cells, we recorded α-cell K2P currents, but we did not detect a difference between WT

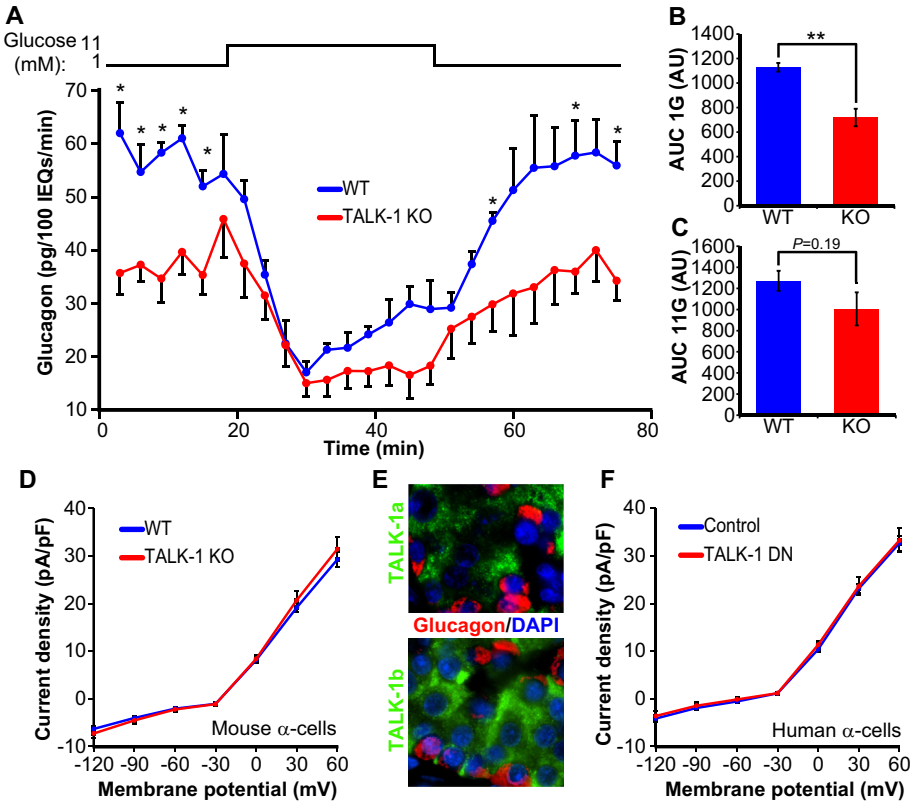

Figure 6: Reduced glucagon secretion from TALK-1 KO islets. (A) Isolated islets from WT and TALK-1 KO mice were perifused with the indicated glucose concentrations ($N = 4$ mice per genotype). (B) Glucagon AUC for the period corresponding to glucagon secretion in 1 mM glucose (0–18 min). (C) Glucagon AUC for the period corresponding to glucagon secretion in 11 mM glucose (18–45 min). (D) K2P current density in WT and TALK-1 KO α-cells ($N = 3$ mice per genotype). (E) Human pancreas sections stained for TALK-1 using two different antibodies and glucagon. (F) K2P current density in human α-cells expressing either TALK-1 DN mutant or mCherry control. Cells were post-stained for glucagon; only glucagon-positive cells were analyzed ($N = 10$ α-cells per condition/five donors); $^{*}P < 0.05$; $^{**}P < 0.005$.

and TALK-1 KO α-cells (Figure 6D). Immunofluorescent analysis of human pancreas sections using two different TALK-1 antibodies failed to demonstrate TALK-1 in α-cells (Figure 6E), and expression of the TALK-1 DN mutant in human α-cells (confirmed by post-staining) had no effect on K2P currents (Figure 6F). As TALK-1 channels are not expressed in α-cells, it is likely that reduced glucagon secretion from TALK-1 KO islets was due to paracrine effects. While insulin is a paracrine inhibitor of glucagon secretion [50], insulin secretion from TALK-1 KO islets was indistinguishable from WT islets in 1 mM glucose [21]. This suggests that the reduced glucagon secretion observed in TALK-1 KO islets is a consequence of increased somatostatin secretion.

Somatostatin receptor signaling inhibits α-cell function through multiple mechanisms, including reduction of cellular cAMP levels [50], suppression of glucagon granule exocytosis [51], and activation of V_m-hyperpolarizing K^+ currents [52–54]. As V_m hyperpolarization limits α-cell Ca^{2+} influx and glucagon secretion [55], we hypothesized that increased basal somatostatin release in TALK-1 KO islets would impact α-cell Ca^{2+}_c dynamics. We tested this possibility by measuring α-cell Ca^{2+}_c oscillations in WT and TALK-1 KO islets, using mice which express the genetically encoded Ca^{2+} indicator GCaMP3 specifically in α-cells [34]. In agreement with findings that somatostatin suppresses α-cell electrical activity and increases in Ca^{2+}_c [54,56], we found that significantly fewer TALK-1 KO α-cells exhibited Ca^{2+}_c oscillations in low (1 mM) glucose when compared to controls (Figure 7A,B, and E). However, disrupting intraislet somatostatin paracrine signaling by dispersing islets into single cells normalized the oscillation frequency of WT and TALK-1 KO α-cells (Figure 7C,D, and E). Similarly, we found a tendency towards lower Ca^{2+}_c in intact islet TALK-1 KO α-cells, a difference which was not found in single TALK-1 KO α-cells (Figure 7F). Single α-cells were still capable of responding to somatostatin, as addition of 10 nM somatostatin caused a transient suppression of Ca^{2+} oscillations (Figure 7C,D), consistent with its effects on α-cell electrical activity [54]. To ascertain the relationship between somatostatin signaling and TALK-1 KO α-cell function, we measured glucagon secretion from WT and TALK-1 KO islets in the presence of the SSTR2 antagonist CYN154806. Blockade of SSTR2, which is the dominant α-cell SSTR [56,57], potently increased glucagon secretion under both low and high glucose conditions and abrogated the reduced glucagon secretion of TALK-1 KO islets (Figure 7G). Together, these findings indicate that TALK-1 modulation of δ-cell somatostatin secretion impacts α-cell Ca^{2+} handling and glucagon secretion.

4. DISCUSSION

Although it is increasingly clear that islet δ-cells serve an important role in glucose homeostasis, our understanding of the mechanisms underlying δ-cell stimulus-secretion coupling has lagged behind that of β- and α-cells. CICR contributes to GSSS [11], but the molecular components which tune δ-cell CICR have remained largely unknown. Recent observations identified TALK-1 channels as important

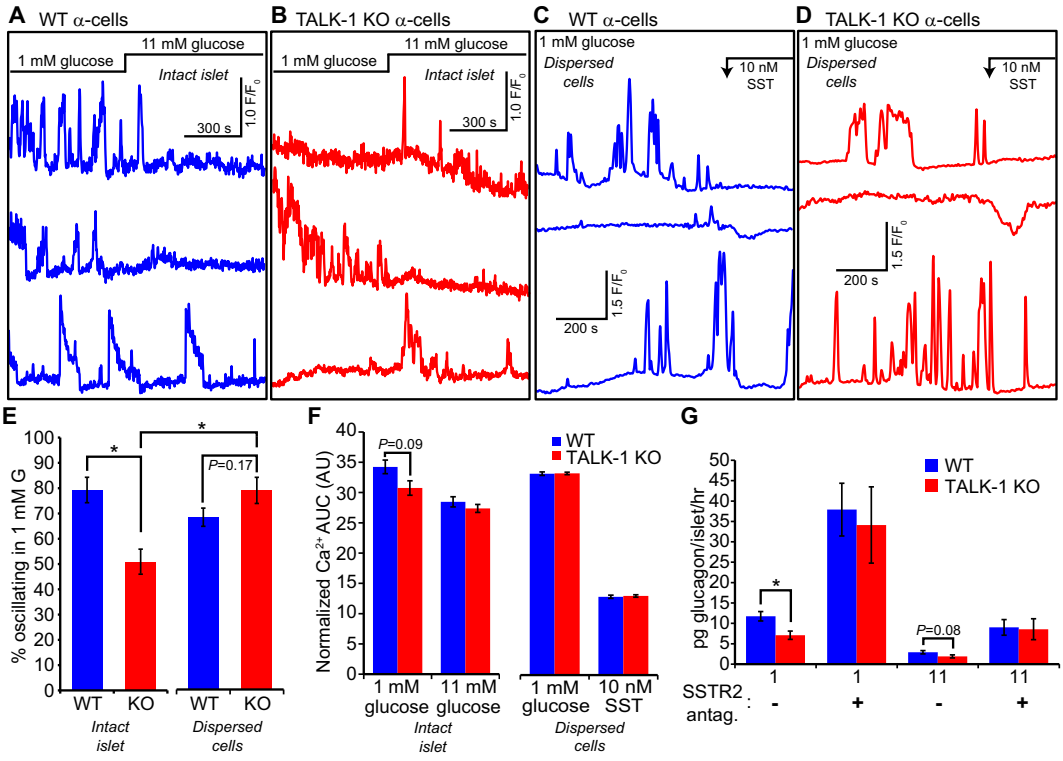

Figure 7: TALK-1 KO α-cells exhibit altered Ca^{2+} dynamics only in intact islets. (A) Recordings of intracellular Ca^{2+} responses in WT α-cells, in islets expressing the genetically encoded Ca^{2+} indicator GCaMP3 specifically in α-cells (representative of islet α-cells from $N = 3$ mice). (B) Recordings of intracellular Ca^{2+} responses in TALK-1 KO α-cells, in islets expressing the genetically encoded Ca^{2+} indicator GCaMP3 specifically in α-cells (representative of islet α-cells from $N = 3$ mice). (C) Recordings of intracellular Ca^{2+} responses in single WT α-cells expressing the genetically encoded Ca^{2+} indicator GCaMP3 (representative of α-cells from $N = 3$ mice). (D) Recordings of intracellular Ca^{2+} responses in single TALK-1 KO α-cells expressing the genetically encoded Ca^{2+} indicator GCaMP3 (representative of α-cells from $N = 3$ mice). (E and F) Comparison of percent oscillating α-cells and Ca^{2+} AUC determined from WT and TALK-1 KO α-cells under the indicated conditions ($N = 3$ mice per genotype). (G) Islets were incubated for 1 h with the indicated treatments (SSTR2 antagonist: 500 nM CYN154806); $N = 10$ mice per genotype (glucose only); 3 mice per genotype (+CYN154806); $^*P < 0.05$.

regulators of β-cell ER Ca^{2+} homeostasis and demonstrated prominent expression of TALK-1 in δ-cells [18,19,22]. Here, we assessed the functional roles of δ-cell TALK-1 channels and examined how TALK-1 modulation of δ-cell somatostatin secretion impacts paracrine regulation of α-cells. Our data suggest that δ-cell TALK-1 channels limit CICR, reducing somatostatin secretion and increasing glucagon release. These observations highlight the importance of CICR during GSSS and demonstrate that TALK-1 channel participate in the regulation of this distinct mode of Ca^{2+} handling.

Ca^{2+} influx through VDCCs is critical for δ-cell exocytosis. Indeed, removal of extracellular Ca^{2+}, V_m hyperpolarization, and pharmacological VDCC blockade all reduce or inhibit δ-cell somatostatin secretion [9–11,58]. While VDCC-mediated Ca^{2+} influx provides the trigger for exocytosis in δ-cells, GSSS is augmented by metabolically enhanced ER Ca^{2+} release [11]. Accordingly, depletion of ER Ca^{2+} (by inhibiting SERCAs) strongly inhibits somatostatin secretion [11,17,58]. The results presented here demonstrate that glucose metabolism augments δ-cell $Ca^{2+}{}_c$ through increased CICR, as hypothesized by Zhang and colleagues [11]. We also found that depletion of ER Ca^{2+} stores significantly blunted depolarization-induced $Ca^{2+}{}_c$ transients, strongly supporting the hypothesis that Ca^{2+} release from the δ-cell ER makes a substantial contribution to GSSS [11]. These data emphasize that metabolic enhancement of δ-cell ER Ca^{2+} stores and subsequent CICR is critical for somatostatin secretion.

Our findings indicate that TALK-1 channels provide a control mechanism for δ-cell ER Ca^{2+} handling and somatostatin secretion. In β-cells TALK-1 channels act as a countercurrent for ER Ca^{2+} leak [22]. The data suggest that TALK-1 may also modulate δ-cell ER Ca^{2+} handling and thereby reduce ER Ca^{2+} content. Similar to β-cells lacking TALK-1, ER Ca^{2+} stores were increased in TALK-1 KO δ-cells, presumably due to reduced ER Ca^{2+} leak [22]. However, despite increased ER Ca^{2+} storage in TALK-1 KO δ-cells, the rate of ER Ca^{2+} release following SERCA inhibition was faster. One possible explanation is that the driving force for ER Ca^{2+} extrusion is increased in response to higher ER Ca^{2+} stores. ER Ca^{2+} stores are also strongly correlated with CICR [14–16], therefore, greater CICR occurs with elevated ER Ca^{2+} storage. The importance of countercurrents in this process is exemplified in muscle cells lacking ER K^+ countercurrents mediated by TRIC-A channels, which results in augmented ER Ca^{2+} stores and enhanced ligand mediated ER Ca^{2+} release (e.g. CICR) [59,60]. An analogous phenotype was found in TALK-1 KO δ-cells, which exhibited significantly higher ER Ca^{2+} stores compared to WT δ-cells and larger glucose- and depolarization-induced $Ca^{2+}{}_c$ transients. Elevated $Ca^{2+}{}_c$ fluctuations in δ-cells lacking TALK-1 channels were normalized by ER Ca^{2+} depletion, demonstrating that increased ER Ca^{2+} release was responsible for augmented TALK-1 KO δ-cell $Ca^{2+}{}_c$ transients. The observation that TALK-1 channels modulate δ-cell ER Ca^{2+} handling is consistent with the role of TALK-1 in limiting ER Ca^{2+} leak in β-cells and underscores the importance of ER Ca^{2+} homeostasis in tuning δ-cell CICR [22].

CICR provides a glucose-dependent mechanism to amplify δ-cell $Ca^{2+}{}_c$ levels and somatostatin secretion, and is conceivably tuned by

ATP-sensitive proteins such as SERCAs and ER Ca^{2+} release channels [11]. The findings presented here suggest that TALK-1 could have multiple effects on δ-cell ER Ca^{2+} homeostasis which influence CICR and somatostatin secretion. As discussed above, TALK-1 channel activity modulates ER Ca^{2+} handling, controlling ER Ca^{2+} levels which determines the driving force for Ca^{2+} to exit the ER. Under conditions of increased ER Ca^{2+} stores, such as in TALK-1 KO δ-cells or in high glucose when SERCAs are energized, elevated ER Ca^{2+} content would be predicted to enhance Ca^{2+} currents through ER Ca^{2+} release channels. In addition, changes in ER Ca^{2+} levels may also shift the sensitivity of δ-cell ER Ca^{2+} handling proteins. For example, the open probability of both ryanodine receptors and inositol trisphosphate receptors are influenced by the free Ca^{2+} concentration in the ER, modulating the sensitivity and magnitude of CICR [61,62]. Therefore, up- or downregulation of TALK-1 channel activity may provide a mechanism to control the dynamic range of δ-cell CICR, scaling Ca^{2+} release and somatostatin secretion to maintain glycemia. It remains to be determined whether gastric δ-cells share the stimulus-secretion mechanisms of islet δ-cells, although TALK-1 is highly expressed in both. Adriaenssens and colleagues found that several incretin hormones elicit Ca^{2+} release from intracellular stores in gastric δ-cells [19], and the findings of this study suggest that TALK-1 channels may serve a role in regulating these responses. Interestingly, one of the few known physiological regulators of TALK-1 currents is extracellular pH [63]. While pH fluctuations around the islet are not expected to be of sufficient magnitude to impact islet cell TALK-1 currents, pH changes in the gastrointestinal tract could regulate gastric δ-cell Ca^{2+} handling and somatostatin secretion. Future studies will define the mechanisms which control the expression and activity of both islet and gastric δ-cell TALK-1 channels to better understand the mechanisms which regulate somatostatin secretion.

TALK-1 modulation of ER Ca^{2+} handling regulates distinct cellular responses in β-cells (e.g., modulation of Ca^{2+}-activated K^+ currents and electrical activity [21,22]) and δ-cells (e.g., control of CICR). While the role of δ-cell TALK-1 channels in CICR-dependent modulation of the V_m is unclear, we found minimal defects in TALK-1 KO δ-cell electrical activity. It is important to note that our V_m recordings of TALK-1 KO δ-cells were performed in clusters of islet cells, whereas our β-cell V_m recordings [21] were performed in intact islets. Under these conditions, paracrine interactions between β-, δ-, and α-cells which affect δ-cell ER Ca^{2+} handling may be perturbed. It is increasingly clear that signaling between β- and δ-cells serves an important function in synchronizing islet hormone secretion, and our findings indicate that islet TALK-1 channels participate in this process. The functional coupling of β- and δ-cells is demonstrated by observations of simultaneous oscillations of insulin and somatostatin release from perfused pancreas [64] as well as synchronized islet β- and δ-cell $Ca^{2+}{}_c$ oscillations [31]. "Chemical coupling" of β- and δ-cells is mediated by the peptide hormone urocortin3 (Ucn3), which is co-released with insulin to stimulate δ-cell type 2 corticotropin releasing hormone receptors (Crhr2) [9]. The effects of Ucn3 on δ-cell Ca^{2+} handling have not been determined, but Crhr2 activation can trigger IP3R-dependent ER Ca^{2+} release in heterologous expression systems and neurons [65,66]. This suggests the possibility that β- to δ-cell signaling incorporates δ-cell ER Ca^{2+} release, the magnitude of which is controlled by TALK-1 channels. In agreement with such a role for ER Ca^{2+} release, we found that depletion of ER Ca^{2+} (via SERCA inhibition) disrupted the coordination of β- and δ-cell $Ca^{2+}{}_c$ oscillations. We also observed an increased frequency of δ-cell $Ca^{2+}{}_c$ oscillations in TALK-1 KO islets, similar to TALK-1 KO β-cells. This phenotype is likely due to increased β-cell electrical and $Ca^{2+}{}_c$ oscillations [21], as we found no difference between WT and TALK-1 KO δ-cell $Ca^{2+}{}_c$ oscillation frequency in low glucose when β-cells are quiescent. In addition to a possible alteration in chemical coupling between TALK-1 KO β- and δ-cells, TALK-1 may also influence electrical coupling between β- and δ-cells; indeed, gap junctions have been detected between β- and δ-cells [67–69]. Although the mechanisms and hierarchy of β- and δ-cell functional coupling remain to be determined, TALK-1 control of the integration of inputs from β- and δ-cells likely serves an important role in modulating glucagon secretion.

Inhibition of islet TALK-1 channel activity inhibits glucagon secretion while stimulating insulin and somatostatin secretion. Therefore, inhibition of TALK-1 channels could be beneficial in patients with T2DM. Indeed, TALK-1 KO mice fed a high-fat diet exhibit reduced fasting glycemia [21]. The findings described here suggest that the lower fasting glycemia in TALK-1 KO mice may arise due to elevated somatostatin secretion and reduced glucagon secretion, in addition to increased insulin secretion. Increased glucagon secretion at 1 mM glucose in the presence of an SSTR2 inhibitor highlights the importance of δ-cell paracrine signaling to the inhibitory action of TALK-1 on glucagon secretion. While the basis for this effect remains to be determined, it is likely related to decreased α-cell $Ca^{2+}{}_c$ and cAMP levels. SSTR2 signaling in α-cells inhibits adenylyl cyclase synthesis of cAMP and also activates G protein-coupled inwardly-rectifying K^+ channels, which hyperpolarize V_m and inhibit VDCCs [70]. Interestingly, SSTR2 signaling has been shown to reduce α-cell cAMP only at low glucose [71]. Our observations together with these previously published data highlight that α-cells are very sensitive to somatostatin at low glucose, but that alternate mechanisms predominate at high glucose. Taken together, these data also indicate that defects that lead to increases in TALK-1 channel activity may contribute to fasting hyperglycemia under metabolically stressful conditions. In agreement with this hypothesis, a gain-of-function polymorphism in TALK-1 (rs1535500, encoding TALK-1 A277E) is associated with an increased risk for T2DM [24,25,27]. This polymorphism would be predicted to reduce ER Ca^{2+} levels [22]. In δ-cells, increased TALK-1 channel activity would diminish CICR and lower somatostatin secretion. In turn, decreased somatostatin secretion would be expected to increase glucagon secretion and contribute to hyperglycemia. In addition, rs1535500-induced defects in β-cell function may impair β-cell to δ-cell signaling, further contributing to hyperglycemia by allowing inappropriately elevated glucagon secretion. Further studies are needed to understand TALK-1 regulation of δ-cells and the intraislet feedback mechanisms which contribute to glucose control in health and disease.

In conclusion, this study reveals that TALK-1 channels serve a key role in shaping δ-cell $Ca^{2+}{}_c$ and controlling somatostatin secretion by modulating δ-cell ER Ca^{2+} handling. We find that TALK-1 channel activity regulates δ-cell CICR, limiting elevations in $Ca^{2+}{}_c$ and somatostatin secretion. Our data also suggest that defects which lead to increases in TALK-1 channel activity (such as those induced by rs1535500) may participate in the pathogenesis of T2DM by negatively impacting δ-cell function, contributing to elevated glucagon release. These observations improve our understanding of the molecular mechanisms controlling δ-cell stimulus-secretion coupling and highlight the potential clinical utility of TALK-1 channels as a therapeutic target to reduce elevated glucagon secretion in patients with T2DM.

ACKNOWLEDGEMENTS

We thank Professor Anders Tengholm (Department of Medical Cell Biology, Uppsala University, Sweden) for generously providing the Psst-mCherry adenovirus. This

project was funded by National Institutes of Health grants K01DK081666, R01DK097392, Vanderbilt Diabetes Research and Training Center Pilot and Feasibility Grant P60DK20593, and American Diabetes Association grant 1-17-IBS-024 (DAJ); Vanderbilt Molecular Endocrinology Training Program (METP) grant 5T32DK07563 and National Institutes of Health grant 1F31DK109625 (NCV); and Vanderbilt METP grant 5T32DK007563-28 (MKA). The Vanderbilt Translational Pathology Shared Resource assisted in the preparation and processing of paraffin-embedded pancreata (2P30 CA068485-14; 5U24DK059637-13). Confocal microscopy was performed using the Vanderbilt Cell Imaging Shared Resource (DK020593).

AUTHOR CONTRIBUTIONS

NCV and DAJ conceived the project; NCV, MTD, KLJ, PKD, KAK, MKA, SCM, and DAJ performed experiments and analyzed the data; NCV, MTD, and DAJ wrote and edited the manuscript.

CONFLICT OF INTEREST

The authors declare no conflict of interest.

APPENDIX A. SUPPLEMENTARY DATA

Supplementary data related to this article can be found at https://doi.org/10.1016/j.molmet.2018.01.016.

REFERENCES

[1] Patel, Y.C., 1999. Somatostatin and its receptor family. Frontiers in Neuroendocrinology 20(3):157—198.

[2] Hauge-Evans, A.C., King, A.J., Carmignac, D., Richardson, C.C., Robinson, I.C., Low, M.J., et al., 2009. Somatostatin secreted by islet δ-cells fulfills multiple roles as a paracrine regulator of islet function. Diabetes 58(2):403—411.

[3] Cheng-Xue, R., Gomez-Ruiz, A., Antoine, N., Noel, L.A., Chae, H.Y., Ravier, M.A., et al., 2013. Tolbutamide controls glucagon release from mouse islets differently than glucose: involvement of K(ATP) channels from both alpha-cells and delta-cells. Diabetes 62(5):1612—1622.

[4] Nilsson, T., Arkhammar, P., Rorsman, P., Berggren, P.O., 1989. Suppression of insulin release by galanin and somatostatin is mediated by a G-protein. An effect involving repolarization and reduction in cytoplasmic free Ca^{2+} concentration. Journal of Biological Chemistry 264(2):973—980.

[5] Efendic, S., Nylen, A., Roovete, A., Uvnas-Wallenstein, K., 1978. Effects of glucose and arginine on the release of immunoreactive somatostatin from the isolated perfused rat pancreas. FEBS Letters 92(1):33—35.

[6] Brereton, M.F., Vergari, E., Zhang, Q., Clark, A., 2015. Alpha-, delta-and PP-cells: are they the architectural cornerstones of islet structure and co-ordination. Journal of Histochemistry and Cytochemistry 63(8):575—591.

[7] Girard, J., 2017. Glucagon, a key factor in the pathophysiology of type 2 diabetes. Biochimie.

[8] Segerstolpe, Å., Palasantza, A., Eliasson, P., Andersson, E.-M., Andréasson, A.-C., Sun, X., et al., 2016. Single-cell transcriptome profiling of human pancreatic islets in health and type 2 diabetes. Cell Metabolism 24(4):593—607.

[9] van der Meulen, T., Donaldson, C.J., Caceres, E., Hunter, A.E., Cowing-Zitron, C., Pound, L.D., et al., 2015. Urocortin3 mediates somatostatin-dependent negative feedback control of insulin secretion. Nature Medicine 21(7):769—776.

[10] Efendic, S., Grill, V., Nylen, A., Ostensson, C.G., 1982. Difference in calcium dependency of insulin, glucagon and somatostatin secretion in response to glibenclamide in perfused rat pancreas. Diabetologia 22(6):475—479.

[11] Zhang, Q., Bengtsson, M., Partridge, C., Salehi, A., Braun, M., Cox, R., et al., 2007. R-type Ca(2+)-channel-evoked CICR regulates glucose-induced somatostatin secretion. Nature Cell Biology 9(4):453—460.

[12] Braun, M., Ramracheya, R., Amisten, S., Bengtsson, M., Moritoh, Y., Zhang, Q., et al., 2009. Somatostatin release, electrical activity, membrane currents and exocytosis in human pancreatic delta cells. Diabetologia 52(8):1566—1578.

[13] Berts, A., Ball, A., Dryselius, G., Gylfe, E., Hellman, B., 1996. Glucose stimulation of somatostatin-producing islet cells involves oscillatory Ca^{2+} signaling. Endocrinology 137(2):693—697.

[14] Nelson, T.E., Nelson, K.E., 1990. Intra- and extraluminal sarcoplasmic reticulum membrane regulatory sites for Ca2(+)-induced Ca^{2+} release. FEBS Letters 263(2):292—294.

[15] Gyorke, S., Terentyev, D., 2008. Modulation of ryanodine receptor by luminal calcium and accessory proteins in health and cardiac disease. Cardiovascular Research 77(2):245—255.

[16] Missiaen, L., De Smedt, H., Droogmans, G., Casteels, R., 1992. Ca^{2+} release induced by inositol 1,4,5-trisphosphate is a steady-state phenomenon controlled by luminal Ca^{2+} in permeabilized cells. Nature 357(6379):599—602.

[17] Vieira, E., Salehi, A., Gylfe, E., 2007. Glucose inhibits glucagon secretion by a direct effect on mouse pancreatic alpha cells. Diabetologia 50(2):370—379.

[18] Li, J., Klughammer, J., Farlik, M., Penz, T., Spittler, A., Barbieux, C., et al., 2016. Single-cell transcriptomes reveal characteristic features of human pancreatic islet cell types. EMBO Reports 17(2):178—187.

[19] Adriaenssens, A., Lam, B.Y., Billing, L., Skeffington, K., Sewing, S., Reimann, F., et al., 2015. A transcriptome-led exploration of molecular mechanisms regulating somatostatin-producing D-cells in the gastric epithelium. Endocrinology 156(11):3924—3936.

[20] Adriaenssens, A.E., Svendsen, B., Lam, B.Y., Yeo, G.S., Holst, J.J., Reimann, F., et al., 2016. Transcriptomic profiling of pancreatic alpha, beta and delta cell populations identifies delta cells as a principal target for ghrelin in mouse islets. Diabetologia 59(10):2156—2165.

[21] Vierra, N.C., Dadi, P.K., Jeong, I., Dickerson, M., Powell, D.R., Jacobson, D.A., 2015. Type 2 diabetes-associated K^+ channel TALK-1 modulates beta-cell electrical excitability, second-phase insulin secretion, and glucose homeostasis. Diabetes 64(11):3818—3828.

[22] Vierra, N.C., Dadi, P.K., Milian, S.C., Dickerson, M., Jordan, K.L., Gilon, P., et al., 2017. TALK-1 channels control β-cell endoplasmic reticulum Ca^{2+} homeostasis Sci Signal.

[23] Dadi, P.K., Vierra, N.C., Ustione, A., Piston, D.W., Colbran, R.J., Jacobson, D.A., 2014. Inhibition of pancreatic beta-cell Ca^{2+}/calmodulin-dependent protein kinase II reduces glucose-stimulated calcium influx and insulin secretion, impairing glucose tolerance. Journal of Biological Chemistry 289(18):12435—12445.

[24] Cho, Y.S., Chen, C.H., Hu, C., Long, J., Ong, R.T., Sim, X., et al., 2012. Meta-analysis of genome-wide association studies identifies eight new loci for type 2 diabetes in east Asians. Nature Genetics 44(1):67—72.

[25] Replication, D.I.G, Meta-analysis, C, Asian Genetic Epidemiology Network Type 2 Diabetes, C, South Asian Type 2 Diabetes, C, Mexican American Type 2 Diabetes, C, Type 2 Diabetes Genetic Exploration by Next-generation sequencing in muylti-Ethnic Samples, C, et al., 2014. Genome-wide trans-ancestry meta-analysis provides insight into the genetic architecture of type 2 diabetes susceptibility. Nature Genetics 46(3):234—244.

[26] Wood, A.R., Jonsson, A., Jackson, A.U., Wang, N., van Leewen, N., Palmer, N.D., et al., 2017. A genome-wide association study of IVGTT-based measures of first phase insulin secretion refines the underlying physiology of type 2 diabetes variants. Diabetes.

[27] Muller, Y.L., Piaggi, P., Chen, P., Wiessner, G., Okani, C., Kobes, S., et al., 2016. Assessing variation across eight established east asian loci for type 2 diabetes in american indians: suggestive evidence for new sex-specific diabetes signals in GLIS3 and ZFAND3. Diabetes Metabolism Research Review.

[28] Taniguchi, H., He, M., Wu, P., Kim, S., Paik, R., Sugino, K., et al., 2011. A resource of Cre driver lines for genetic targeting of GABAergic neurons in cerebral cortex. Neuron 71(6):995–1013.

[29] Luche, H., Weber, O., Nageswara Rao, T., Blum, C., Fehling, H.J., 2007. Faithful activation of an extra-bright red fluorescent protein in "knock-in" Cre-reporter mice ideally suited for lineage tracing studies. European Journal of Immunology 37(1):43–53.

[30] Roe, M.W., Philipson, L.H., Frangakis, C.J., Kuznetsov, A., Mertz, R.J., Lancaster, M.E., et al., 1994. Defective glucose-dependent endoplasmic reticulum Ca^{2+} sequestration in diabetic mouse islets of Langerhans. Journal of Biological Chemistry 269(28):18279–18282.

[31] Shuai, H., Xu, Y., Yu, Q., Gylfe, E., Tengholm, A., 2016. Fluorescent protein vectors for pancreatic islet cell identification in live-cell imaging. Pflugers Archiv 468(10):1765–1777.

[32] Li, J., Shuai, H., Gylfe, E., Tengholm, A., 2013. Oscillations of sub-membrane ATP in glucose-stimulated beta cells depend on negative feedback from Ca^{2+}. Diabetologia 56(7):1577–1586.

[33] Zhu, L., Almaca, J., Dadi, P.K., Hong, H., Sakamoto, W., Rossi, M., et al., 2017. beta-arrestin-2 is an essential regulator of pancreatic beta-cell function under physiological and pathophysiological conditions. Nature Communications 8:14295.

[34] Dadi, P.K., Luo, B., Vierra, N.C., Jacobson, D.A., 2015. TASK-1 potassium channels limit pancreatic alpha-cell calcium influx and glucagon secretion. Molecular Endocrinology 29(5):777–787.

[35] DiGruccio, M.R., Mawla, A.M., Donaldson, C.J., Noguchi, G.M., Vaughan, J., Cowing-Zitron, C., et al., 2016. Comprehensive alpha, beta and delta cell transcriptomes reveal that ghrelin selectively activates delta cells and promotes somatostatin release from pancreatic islets. Molecular Metabolism 5(7):449–458.

[36] Molina, J., Rodriguez-Diaz, R., Fachado, A., Jacques-Silva, M.C., Berggren, P.O., Caicedo, A., 2014. Control of insulin secretion by cholinergic signaling in the human pancreatic islet. Diabetes 63(8):2714–2726.

[37] Madisen, L., Garner, A.R., Shimaoka, D., Chuong, A.S., Klapoetke, N.C., Li, L., et al., 2015. Transgenic mice for intersectional targeting of neural sensors and effectors with high specificity and performance. Neuron 85(5):942–958.

[38] Kilimnik, G., Jo, J., Periwal, V., Zielinski, M.C., Hara, M., 2012. Quantification of islet size and architecture. Islets 4(2):167–172.

[39] Beck, A., Zur Nieden, R., Schneider, H.-P., Deitmer, J.W., 2004. Calcium release from intracellular stores in rodent astrocytes and neurons in situ. Cell Calcium 35(1):47–58.

[40] Dyachok, O., Gylfe, E., 2001. Store-operated influx of Ca^{2+} in pancreatic β-cells exhibits graded dependence on the filling of the endoplasmic reticulum. Journal of Cell Science 114(11):2179–2186.

[41] Brini, M., Bano, D., Manni, S., Rizzuto, R., Carafoli, E., 2000. Effects of PMCA and SERCA pump overexpression on the kinetics of cell Ca 2+ signalling. The EMBO Journal 19(18):4926–4935.

[42] Solovyova, N., Veselovsky, N., Toescu, E., Verkhratsky, A., 2002. Ca^{2+} dynamics in the lumen of the endoplasmic reticulum in sensory neurons: direct visualization of Ca^{2+}-induced Ca^{2+} release triggered by physiological Ca^{2+} entry. The EMBO Journal 21(4):622–630.

[43] Gilon, P., Arredouani, A., Gailly, P., Gromada, J., Henquin, J.C., 1999. Uptake and release of Ca^{2+} by the endoplasmic reticulum contribute to the oscillations of the cytosolic Ca^{2+} concentration triggered by Ca^{2+} influx in the electrically excitable pancreatic B-cell. Journal of Biological Chemistry 274(29):20197–20205.

[44] Beauvois, M.C., Arredouani, A., Jonas, J.C., Rolland, J.F., Schuit, F., Henquin, J.C., et al., 2004. Atypical Ca2+-induced Ca2+ release from a sarco-endoplasmic reticulum Ca2+-ATPase 3-dependent Ca2+ pool in mouse pancreatic β-cells. The Journal of Physiology 559(1):141–156.

[45] Dyachok, O., Gylfe, E., 2004. Ca^{2+}-induced Ca^{2+} release via inositol 1, 4, 5-trisphosphate receptors is amplified by protein kinase A and triggers exocytosis in pancreatic β-cells. Journal of Biological Chemistry 279(44):45455–45461.

[46] Li, J., Yu, Q., Ahooghalandari, P., Gribble, F.M., Reimann, F., Tengholm, A., et al., 2015. Submembrane ATP and Ca^{2+} kinetics in alpha-cells: unexpected signaling for glucagon secretion. The FASEB Journal 29(8):3379–3388.

[47] Zhang, Q., Ramracheya, R., Lahmann, C., Tarasov, A., Bengtsson, M., Braha, O., et al., 2013. Role of K_{ATP} channels in glucose-regulated glucagon secretion and impaired counterregulation in type 2 diabetes. Cell Metabolism 18(6):871–882.

[48] Blodgett, D.M., Nowosielska, A., Afik, S., Pechhold, S., Cura, A.J., Kennedy, N.J., et al., 2015. Novel observations from next generation RNA sequencing of highly purified human adult and fetal islet cell subsets. Diabetes db150039.

[49] Xin, Y., Kim, J., Okamoto, H., Ni, M., Wei, Y., Adler, C., et al., 2016. RNA sequencing of single human islet cells reveals type 2 diabetes genes. Cell Metabolism 24(4):608–615.

[50] Elliott, A.D., Ustione, A., Piston, D.W., 2015. Somatostatin and insulin mediate glucose-inhibited glucagon secretion in the pancreatic alpha-cell by lowering cAMP. American Journal of Physiology. Endocrinology and Metabolism 308(2):E130–E143.

[51] Gromada, J., Hoy, M., Buschard, K., Salehi, A., Rorsman, P., 2001. Somatostatin inhibits exocytosis in rat pancreatic alpha-cells by G(i2)-dependent activation of calcineurin and depriming of secretory granules. The Journal of Physiology 535(Pt 2):519–532.

[52] Yoshimoto, Y., Fukuyama, Y., Horio, Y., Inanobe, A., Gotoh, M., Kurachi, Y., 1999. Somatostatin induces hyperpolarization in pancreatic islet alpha cells by activating a G protein-gated K^+ channel. FEBS Letters 444(2–3):265–269.

[53] Gromada, J., Hoy, M., Olsen, H.L., Gotfredsen, C.F., Buschard, K., Rorsman, P., et al., 2001. Gi2 proteins couple somatostatin receptors to low-conductance K^+ channels in rat pancreatic alpha-cells. Pflugers Archiv 442(1):19–26.

[54] Ramracheya, R., Ward, C., Shigeto, M., Walker, J.N., Amisten, S., Zhang, Q., et al., 2010. Membrane potential-dependent inactivation of voltage-gated ion channels in alpha-cells inhibits glucagon secretion from human islets. Diabetes 59(9):2198–2208.

[55] Le Marchand, S.J., Piston, D.W., 2012. Glucose decouples intracellular Ca^{2+} activity from glucagon secretion in mouse pancreatic islet alpha-cells. PLoS One 7(10):e47084.

[56] Kailey, B., van de Bunt, M., Cheley, S., Johnson, P.R., MacDonald, P.E., Gloyn, A.L., et al., 2012. SSTR2 is the functionally dominant somatostatin receptor in human pancreatic beta- and alpha-cells. American Journal of Physiology. Endocrinology and Metabolism 303(9):E1107–E1116.

[57] Strowski, M.Z., Parmar, R.M., Blake, A.D., Schaeffer, J.M., 2000. Somatostatin inhibits insulin and glucagon secretion via two receptors subtypes: an in vitro study of pancreatic islets from somatostatin receptor 2 knockout mice. Endocrinology 141(1):111–117.

[58] Li, Q., Cui, M., Yang, F., Li, N., Jiang, B., Yu, Z., et al., 2017. A cullin 4B-RING E3 ligase complex fine-tunes pancreatic delta cell paracrine interactions. Journal of Clinical Investigation.

[59] Zhao, X., Yamazaki, D., Park, K.H., Komazaki, S., Tjondrokoesoemo, A., Nishi, M., et al., 2010. Ca^{2+} overload and sarcoplasmic reticulum instability in tric-a null skeletal muscle. Journal of Biological Chemistry 285(48):37370–37376.

[60] Yamazaki, D., Tabara, Y., Kita, S., Hanada, H., Komazaki, S., Naitou, D., et al., 2011. TRIC-A channels in vascular smooth muscle contribute to blood pressure maintenance. Cell Metabolism 14(2):231–241.

[61] Laver, D.R., 2007. Ca^{2+} stores regulate ryanodine receptor Ca^{2+} release channels via luminal and cytosolic Ca^{2+} sites. Biophysical Journal 92(10):3541–3555.

[62] Vais, H., Foskett, J.K., Ullah, G., Pearson, J.E., Mak, D.O., 2012. Permeant calcium ion feed-through regulation of single inositol 1,4,5-trisphosphate receptor channel gating. The Journal of General Physiology 140(6):697–716.

[63] Girard, C., Duprat, F., Terrenoire, C., Tinel, N., Fosset, M., Romey, G., et al., 2001. Genomic and functional characteristics of novel human pancreatic 2P domain K(+) channels. Biochemical and Biophysical Research Communications 282(1):249–256.

[64] Stagner, J.I., Samols, E., Weir, G.C., 1980. Sustained oscillations of insulin, glucagon, and somatostatin from the isolated canine pancreas during exposure to a constant glucose concentration. Journal of Clinical Investigation 65(4):939–942.

[65] Gutknecht, E., Van der Linden, I., Van Kolen, K., Verhoeven, K.F., Vauquelin, G., Dautzenberg, F.M., 2009. Molecular mechanisms of corticotropin-releasing factor receptor-induced calcium signaling. Molecular Pharmacology 75(3): 648–657.

[66] Brailoiu, G.C., Deliu, E., Tica, A.A., Chitravanshi, V.C., Brailoiu, E., 2012. Urocortin 3 elevates cytosolic calcium in nucleus ambiguus neurons. Journal of Neurochemistry 122(6):1129–1136.

[67] Briant, L., Reinbothe, T., Spiliotis, I., Miranda, C., Rodriguez, B., Rorsman, P., 2017. δ-cells and β-cells are electrically coupled and regulate α-cell activity via somatostatin. The Journal of Physiology.

[68] Meda, P., Kohen, E., Kohen, C., Rabinovitch, A., Orci, L., 1982. Direct communication of homologous and heterologous endocrine islet cells in culture. The Journal of Cell Biology 92(1):221–226.

[69] Michaels, R.L., Sheridan, J.D., 1981. Islets of Langerhans: dye coupling among immunocytochemically distinct cell types. Science 214(4522):801–803.

[70] Briant, L., Salehi, A., Vergari, E., Zhang, Q., Rorsman, P., 2016. Glucagon secretion from pancreatic α-cells. Upsala Journal of Medical Sciences 121(2): 113–119.

[71] Tengholm, A., Gylfe, E., 2017. cAMP signaling in insulin and glucagon secretion. Diabetes, Obesity and Metabolism 19:42–53.

